

## Compartmental Diffusion in Breast Cancer

Edna Furman-Haran<sup>1</sup>, Myra Feinberg-Shapiro<sup>2</sup>, Erez Eyal<sup>1</sup>, Dov Grobgeld<sup>1</sup>, Noemi Weisenberg<sup>1</sup>, Noam Nissan<sup>1</sup>, Tania Zehavi<sup>2</sup>, and Hadassa Degani<sup>1</sup>  
<sup>1</sup>The Weizmann Institute of Science, Rehovot, Israel, <sup>2</sup>Meir Medical Center, Kfar Saba, Israel

### Introduction:

Water diffusion in tissues presents a highly complex process as the system is composed of different compartments with partial restriction and hindrance inside and outside these compartments, respectively. Changes in the water diffusion are usually related to variations in the micro/cellular structure and physiology of the underlying tissue, including intravoxel incoherent motion, extracellular tortuosity, restriction by cell membrane, and exchange between tissue compartments. As a first approximation it is possible to describe tissue water diffusion at the cellular level by a two-compartment exchange model comprised of extracellular and intracellular environments (1,2).

In recent years, the evaluation of diffusion weighted imaging (DWI) have shown promise in breast MR as an adjunct method to DCE. In these studies 2 to 5 b-values were applied in the range 0 to 1000 sec/mm<sup>2</sup> (3, and references cited therein) yielding maps of apparent diffusion coefficient (ADC), that are predominantly sensitive to changes in the extracellular diffusion. We have previously investigated water self diffusion in the different microenvironments of orthotopic human breast cancer xenografts in mice by applying a broad range of b-values and using an approximated two compartment model (4,5). More recently we have applied breast diffusion tensor imaging (DTI) in healthy volunteers and breast cancer patients using 2 b-values, 0 and 700 sec/mm<sup>2</sup> (6). The analysis of the DTI datasets yielded maps of the diffusion tensor eigenvectors and eigenvalues, as well as the anisotropic water diffusion indices, demonstrating ability to track the mammary ductal trees and detect their blockage by cancer cells (6,7). In this study we describe the application of an imaging protocol and processing tools for estimating the diffusion parameters characterizing the different compartments in the normal human mammary tissue and in cancerous lesions.

### Methods:

The study was approved by the IRB of Meir Medical Center and included thus far 23 patients with 27 biopsy confirmed breast cancer lesions (12 IDC, 7 ILC and 8 DCIS). Images were acquired on a 3 Tesla Trio scanner (Siemens). The MRI protocol included axial T2 weighted images; DWI with fat suppression with diffusion gradients applied at 3 orthogonal directions or at the read direction, with a fixed TE of 120 msec and 11 b-values in the range 0 to 2200 sec/mm<sup>2</sup>; DTI with fat suppression, with diffusion gradients applied at 30 directions, TE of 120 msec at two b values 0 and 700 sec/mm<sup>2</sup>; and a DCE-MRI protocol (6). 60 slices were acquired with a spatial resolution in the diffusion studies of 1.9x1.9x (2-2.5) mm<sup>3</sup>, covering the entire breasts. The entire imaging time was ~30 minutes.

DTI datasets were analyzed using a propriety software, yielding 3 eigenvectors and their corresponding eigenvalues  $\lambda_1$ ,  $\lambda_2$  and  $\lambda_3$  (3). Results were presented in parametric maps, overlaid on the corresponding T2 or T1 weighted images. ADC values were also calculated according to:  $ADC = (\lambda_1 + \lambda_2 + \lambda_3)/3$ . DWI images were analyzed by assuming a bi-exponential decay:  $S/S_0 = P_f \exp(-bD_f) + P_s \exp(-bD_s)$ , where  $P_f$  and  $P_s$  are the fractions of the fast and slow decay and  $D_f$  and  $D_s$  their corresponding decay constants associated with fast and slow diffusion processes in the extracellular and intracellular compartments, respectively (8). Both pixel-by-pixel and region of interest (ROI) analysis were applied in each central tumor slice. Tumors' ROI were delineated on  $\lambda_1$  maps, using a threshold of  $\lambda_1 < 0.0015$  mm<sup>2</sup>/sec, in correlation with the enhancement in DCE-MRI images. A comparable size region of normal fibroglandular tissue was delineated manually in the other breast. Two pixel by pixel analyses in ROIs of normal and malignant regions were applied: non-linear bi-exponential fitting and separate mono-exponential fitting of low b values (in the range: 0-750 sec/mm<sup>2</sup>) and of high b-values (in the range: 750-2200 sec/mm<sup>2</sup>). The quality of the fits was assessed by correlation coefficient ( $R^2$ ) maps.

### Results and Discussion:

Applying strong diffusion gradients with a constant TE of 120 msec revealed that in malignant lesions signal decay as a function of the diffusion weighting deviates from a simple monoexponential behavior, while in the normal fibroglandular tissue a mono-exponential decay function better describes signal attenuation (Fig. 1). However, due to the low SNR, particularly in images acquired with high b-values, the pixel by pixel bi-exponential fitting failed, in most cases, to yield reliable results. Therefore, we have applied separate mono-exponential fitting for the low and high b-values. Analysis involved linear fitting of the normalized values of the natural logarithm of the signal intensity. The slope of these linear curves yielded  $D_f$  and  $D_s$  (Fig. 1) and extrapolation of the slow decay to  $b=0$  provided an approximate estimation of the intracellular volume fraction.

A pixel-by-pixel analysis of the normalized image intensity as a function of b, using separate monoexponential function fits for the low and high b-values range, yielded diffusion parametric maps associated with the fast  $D_f$  and slow  $D_s$  diffusion rates (Fig. 2).

At the low b-values range the correlation coefficients of the fitting were high ( $R^2 > 0.9$ ) in both cancers and normal tissue. At the high b-values range these coefficients were moderate in cancers ( $R^2 > 0.75$ ), whereas in the normal tissue they were in most regions low. The results indicated that  $\lambda_1$ , ADC and  $D_f$  were lower in the cancerous lesions in comparison to the surrounding normal tissue with a higher uniformity of  $\lambda_1$  in the fibroglandular breast tissue and a better contrast to delineate the cancerous lesion, in comparison to ADC parametric maps. A high similarity was observed between the  $D_f$  maps and the ADC maps, indicating that a protocol with b-values of 0 and 700 sec/mm<sup>2</sup> can approximately describe changes in the extracellular diffusion coefficient, most likely associated with cell density (5).

The slow diffusion coefficients,  $D_s$ , were ~5 times lower than the fast diffusion coefficients, as was previously shown in human breast cancer xenografts in mice for constant diffusion time studies (4,5).

The derived maps provided estimation of the diffusion characteristics of breast cancers as compared to normal breast tissue, reflecting predominantly differences in the density and size of the cells.

**Conclusion:** The various diffusion protocols provide a means for characterizing breast tissue global architecture and cellular structure and can be applied to develop a standalone diffusion protocol for detecting breast cancer.

**References:** 1. Karger J et al. *Adv. Magn. Reson.* 12: 1–89, 1988. 2. Price WS, et al. *Biophys J.* 74:2259-71, 1998. 3. Tsushima Y. et al. *J. Magn. Reson. Imaging*, 30:249-255, 2009. 4. Paran Y. et al. *NMR Biomed.* 17:170-180, 2004. 5. Paran Y. et al. *Isr. J. Chem.* 43: 103–114 (2003). 6. Eyal E. et al. *Invest Radiol.* 47: 284–291 2012. 7. Furman-Haran E. et al. *ISMRM p.515*, 2011. 8. Le Bihan, D. *NMR Biomed.*, 8(7–8): 375–386, 1995.

Supported by Yeda Fund No. KY2010-642; The last author holds the Fred and Andrea Fallek Chair for Breast Cancer Research.

The help of Nachum Stern and Fanny Attar is gratefully acknowledged

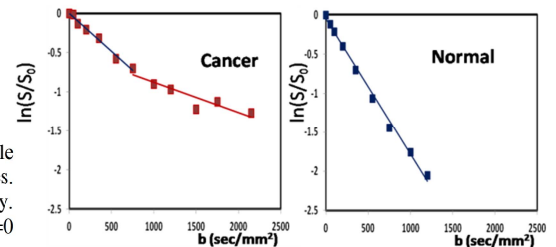


**Fig. 1** Plots of signal attenuation as a function of b value in an ILC lesion and in a normal fibroglandular breast tissue. Note the deviation from a mono-exponential decay in the cancer lesion.

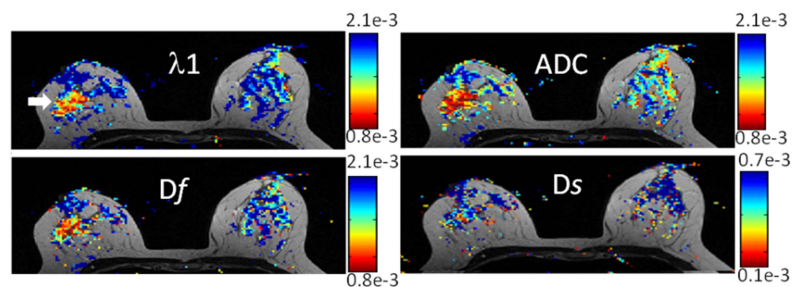


**Fig. 2** Parametric diffusion maps of a breast ILC lesion. The lesion is marked with a white arrow on the  $\lambda_1$  map. The scale is in mm<sup>2</sup>/sec.